

# Modelling of gasoline fuel droplets heating and evaporation

Al Qubeissi, M. , Sazhin, S.S. , Turner, J. , Begg, S. , Crua, C. and Heikal, M.R.

**Author post-print (accepted) deposited in CURVE June 2016**

**Original citation & hyperlink:**

Al Qubeissi, M. , Sazhin, S.S. , Turner, J. , Begg, S. , Crua, C. and Heikal, M.R. (2015) Modelling of gasoline fuel droplets heating and evaporation. Fuel, volume 159 : 373–384.

<http://dx.doi.org/10.1016/j.fuel.2015.06.028>

**Publisher statement:** NOTICE: this is the author's version of a work that was accepted for publication in Fuel. Changes resulting from the publishing process, such as peer review, editing, corrections, structural formatting, and other quality control mechanisms may not be reflected in this document. Changes may have been made to this work since it was submitted for publication. A definitive version was subsequently published in Fuel [Vol 159 (2015)] DOI: 10.1016/j.fuel.2015.06.028.

© 2015, Elsevier. Licensed under the Creative Commons Attribution-NonCommercial-NoDerivatives 4.0 International <http://creativecommons.org/licenses/by-nc-nd/4.0/>

This document is the author's post-print version, incorporating any revisions agreed during the peer-review process. Some differences between the published version and this version may remain and you are advised to consult the published version if you wish to cite from it.

**CURVE is the Institutional Repository for Coventry University**

<http://curve.coventry.ac.uk/open>

# Modelling of gasoline fuel droplets heating and evaporation

M. Al Qubeissi, S.S. Sazhin\*, J. Turner, S. Begg, C. Crua, M.R. Heikal

*Centre for Automotive Engineering, School of Computing Engineering and Mathematics, University of Brighton,  
Brighton BN2 4GJ, United Kingdom*

## Abstract

The paper presents a new approach to modelling of the heating and evaporation of gasoline fuel droplets with a specific application to conditions representative of internal combustion engines. A number of the components of gasoline with identical chemical formulae and close thermodynamic and transport properties are replaced with characteristic components leading to reducing the original composition of gasoline fuel (83 components) to 20 components only. Furthermore, the approximation to the composition of gasoline with these components is replaced with a smaller number of hypothetical quasi-components/components as previously suggested in the multi-dimensional quasi-discrete (MDQD) model. The transient diffusion of quasi-components and single components in the liquid phase as well as the temperature gradient and recirculation inside the droplets, due to the relative velocities between the droplets and the ambient air, are accounted for in the model. In the original MDQD model, n-alkanes and iso-alkanes are considered as one group of alkanes. In this new approach, the contributions of these two groups are taken into account separately. The values for the initial model parameters were selected from experimental data measured in a research engine prior to combustion. The results are compared with the predictions of the single-component model in which the transport and thermodynamic properties of components are averaged, diffusion of species is ignored and liquid thermal conductivity is assumed to be infinitely large, or approximated by those of iso-octane. It is shown that the application of the latter models leads to an under-prediction of the droplet evaporation time by approximately 67% (averaged) and 47% (iso-octane), respectively, compared to those obtained using the discrete component model, taking into account the contributions of 20 components. It is shown that the approximation of the actual composition of gasoline fuel by 6 quasi-components/components, using the MDQD model, leads to an under-prediction of the estimated droplet surface temperatures and evaporation times by approximately 0.9% and 6.6% respectively, for the same engine conditions. The application of the latter model has resulted in an approximately 70% reduction in CPU processor time compared to the model taking into account all 20 components of gasoline fuel.

*Keywords:* Droplet heating, evaporation, hydrocarbon fuel, gasoline fuel

\*Corresponding author, e-mail: [S.Sazhin@brighton.ac.uk](mailto:S.Sazhin@brighton.ac.uk), telephone: +44(0)1273 642677

# 1. Introduction

Gasoline is a fuel widely used in internal combustion engines [1–4]. It is a middle distillate of petroleum, mainly containing C4-C12 hydrocarbons [1,2]. Gasoline fuel droplet heating and evaporation are critical phases in the mixture preparation process that is central to optimum combustion engine efficiency. The accuracy in modelling of these processes has become increasingly important in improving and validating the performance of these combustion systems (e.g. stratified charge, direct injection etc.) [3,5,6]. There have been several approaches to accurate modelling of fuel droplet heating and evaporation [7–16]. In many studies, gasoline fuels are approximated with iso-octane (2,2,4-trimethylpentane structure) (see [17–19]); while realistic gasoline fuels include tens of numbers of hydrocarbons [20]. A typical example of a gasoline fuel composition used as Fuel for Advanced Combustion Engines (FACE C) is shown in Table 1 (see [2] for the details of other compositions of FACE gasoline fuels).

Two main approaches have been used for the analysis of fuel droplet heating and evaporation taking into account its multi-component composition. The first approach is based on the analysis of individual components, the Discrete Component (DC) model [21–28], that is generally applicable to the cases when relatively small numbers of components need to be taken into account. The second approach is based on the probabilistic analysis of a large number of components. This approach has been used in the continuous thermodynamics [29–36] and the distillation curve [37–39] models. In the second approach a number of additional simplifying assumptions have been used, including the assumption that species inside droplets either mix infinitely quickly (infinite diffusivity (ID) model) or do not mix at all (single-component (SC) model). In addition, the temperature gradients inside the droplets have been ignored in most cases by assuming that the liquid thermal conductivity is infinitely large (infinite thermal conductivity (ITC) model). These assumptions have been considered too approximate for the modelling of representative automotive fuel droplets, heating and evaporation [3,8,11,12,40,41]. As a compromise, several modelling approaches combining the benefits of the two aforementioned approaches, were suggested in [35,42–44]. **Apart from these approaches a number of authors (e.g. [45,46]) focused their analyses on the numerical solutions of the full Navier-Stokes equations for multi-component droplets. It is not feasible at the moment, however, to use such approach in modelling realistic fuel sprays in internal combustion engines, taking into account all complexities of fluid dynamics, heat/mass transfer and combustion processes.**

A new model for the heating and evaporation of multi-component fuel droplets, known as the multi-dimensional quasi-discrete (MDQD) model, was introduced in [13]. This model is based on further development of the ideas described in [8,12], where the so called quasi-discrete model was suggested and tested. In the MDQD

32 model a large number (up to about one hundred) of components have been replaced with a smaller number of  
33 quasi-components/components, taking into account the contributions of various groups of species (apart from  
34 alkanes) in representative Diesel fuel droplets. The quasi-components have been introduced as hypothetical spe-  
35 cies with non-integer numbers of carbon and hydrogen atoms (see [8,12] for further details). In our analysis  
36 here, the MDQD model has been applied to the analysis of gasoline fuel droplets. In contrast to [13,47], the con-  
37 tributions of the two groups of alkanes, n-alkanes (n-paraffin) and iso-alkanes (iso-paraffin), are considered sep-  
38 arately, taking into account the differences in their thermodynamic and transport properties.

39 In the following section, the composition of FACE gasoline fuel used in our paper is described. The main fea-  
40 tures of the model used in our analysis are summarised in Section 3. The results of calculations are presented in  
41 Section 4, and the main results of the paper are summarised in Section 5.

## 42 2. Composition of gasoline fuel

43 Our analysis is focused on FACE-C gasoline fuel, the normalised composition of which is shown in Table 1  
44 [1] where the unidentified components (with up to 0.087% of total molar fractions) are ignored. Data presented  
45 in this table are close to average contributions of species for several types of gasoline fuels [20].

46 Note that some components shown in Table 1 have similar carbon numbers, chemical formulae and thermo-  
47 dynamic and transport properties. The main differences between these components are their molecular struc-  
48 tures, as illustrated for some molecules in Fig. 1. This allows us to replace these groups of similar components  
49 with single components (with averaged properties, based on averaged molar weights; or the ones with the high-  
50 est molar contributions in the groups with molar fractions up to 1.5%); see the penultimate column in Table 1.  
51 This approach allows us to reduce the number of species in gasoline fuel to 20 components. These components  
52 are allocated to 3 groups, n-alkanes (5 components), iso-alkanes (8 components), and aromatics (4 components);  
53 and 3 components approximating groups with small molar fractions (indanes/naphthalenes, cycloalkanes and  
54 olefins). Molar fractions of these groups and components are shown in Table 2.

## 55 3. Model

56 Following [11,13,16,40,48,49], the analyses are based on the assumption that droplets are spherically sym-  
57 metric; the temperature gradient and species diffusions in the liquid phase and the effect of internal recirculation  
58 due to the relative velocity between the ambient gas and droplets are taken into account. The effects of coupling  
59 between gas and droplets are ignored (see [50] for a possible approach to take into account this effect).

60 The previously developed multi-dimensional quasi-discrete (MDQD) model, in which the actual composition  
61 of fuel is reduced to a much smaller number of representative quasi-components/components (QC/C), is used in

62 our analysis. In this model, the effects of finite liquid thermal conductivity, QC/C diffusivity and recirculation are  
63 taken into account using the Effective Thermal Conductivity and Effective Diffusivity (ETC/ED) models. The  
64 analyses are based on the previously obtained analytical solutions to the heat transfer and species diffusion  
65 equations within droplets (see [6,10,51–53]). In contrast to [13,47], where the MDQD model was applied to 9  
66 groups of components, our analysis is focused on 6 groups (shown in Table 2). Three of these groups are approx-  
67 imated by single components, while QC are generated for three remaining groups of alkanes: n-alkanes (n-  
68 paraffins), iso-alkanes (i-paraffins) and aromatics. For each group  $m$  ( $m= 1$  to 3), the values of carbon numbers  
69  $\bar{n}_{jm}$  for QC can be introduced, following [13], as:

$$\begin{aligned}
70 \quad \bar{n}_{1m} &= \frac{\sum_{n=n_{1m}}^{n=n(\varphi_m+1)m} (nX_{nm})}{\sum_{n=n_{1m}}^{n=n(\varphi_m+1)m} X_{nm}}, \\
71 \quad \bar{n}_{2m} &= \frac{\sum_{n=n(\varphi_m+2)}^{n=n(2\varphi_m+2)m} (nX_{nm})}{\sum_{n=n(\varphi_m+2)}^{n=n(2\varphi_m+2)m} X_{nm}}, \\
72 \quad \bar{n}_{3m} &= \frac{\sum_{n=n(2\varphi_m+3)}^{n=n(3\varphi_m+3)m} (nX_{nm})}{\sum_{n=n(2\varphi_m+3)}^{n=n(3\varphi_m+3)m} X_{nm}}, \\
73 \quad &\vdots \\
74 \quad \bar{n}_{lm} &= \frac{\sum_{n=n((\ell-1)\varphi_m+\ell)m}^{n=nk_m} (nX_{nm})}{\sum_{n=n((\ell-1)\varphi_m+\ell)m}^{n=nk_m} X_{nm}},
\end{aligned} \tag{1}$$

75 where  $X_{nm}$  are molar fractions of components with carbon number  $n$  within the group  $m$ ,  $n_{1m} = n_{m(\min)}$  is the  
76 minimal value of  $n$  in group  $m$ ,  $n_{km} = n_{m(\max)}$  is the maximal value of  $n$  in group  $m$ ,  $\ell = \text{integer}((k_m + \varphi_m)/$   
77  $(\varphi_m + 1))$ ,  $\varphi_m + 1$  is equal to the number of components to be included within each quasi-component.  $k_m$  is the  
78 number of components within each group  $m$ ,  $\varphi_m$  is assumed to be the same for all QC within group  $m$ . If  $\varphi_m = 0$   
79 then  $\ell = k_m$  and the number of QC is equal to the number of actual components.

80 The number of components contributing within each QC ( $n_{cm}$ ), except possibly the last one, could be taken  
81 equal to the nearest integer of the ratio  $n_{km}/n_{qm}$ , where  $n_{qm}$  is the number of quasi-components in each group  
82  $m$ . As in the case of the original MDQD model,  $\bar{n}_{im}$  are not integers in the general case. Note that the above ap-  
83 proach cannot be applied in the case when  $n_{qm}$  are close to the numbers of components in each group. In this  
84 case, some components within groups form quasi-components, while other components are considered sepa-  
85 rately. In this case a mixture of quasi-components/components (QC/C) is formed in such a way that the molar  
86 fractions of these QC/C are as close as possible. This approach is used in our analysis.

87

88 As in [13], the molar fractions of quasi-components are estimated as:

$$\begin{aligned}
89 \quad X_{1m} &= \sum_{n=n_{1m}}^{n=n_{(\varphi_m+1)m}} X_{nm}, \\
90 \quad X_{2m} &= \sum_{n=n_{(\varphi_m+2)m}}^{n=n_{(2\varphi_m+2)m}} X_{nm}, \\
91 \quad &\vdots \\
92 \quad X_{lm} &= \sum_{n=n_{((\ell-1)\varphi_m+\ell)m}}^{n=n_{km}} X_{nm},
\end{aligned} \tag{2}$$

93 As in [13,47], the mixtures are treated as ideal (Raoult's law is assumed to be valid [54]). In this case, partial  
94 pressures of individual quasi-components/components (QC/C) are estimated as:

$$95 \quad p_v(\bar{n}_{im}) = X_{l_{sim}}(\bar{n}_{im}) p^{sat}(\bar{n}_{im}), \tag{3}$$

96 where  $X_{l_{sim}}$  are the molar fractions of liquid QC/C at the surface of the droplet,  $p^{sat}(\bar{n}_{im})$  are calculated from the  
97 data presented in Appendices A-D. As assumed in our previous studies (e.g. [8,12,13,55]), gasoline fuel vapour  
98 diffuses from the surface of the droplet, without changing its composition, based on averaged binary diffusion of  
99 fuel into dry air. The gasoline fuel vapour is replaced with the vapour of iso-octane; the binary diffusion coeffi-  
100 cient is estimated using the following expression [56]:

$$101 \quad D_{va} = (A + B T + C T^2) \times 10^{-4} \text{ (m}^2 \text{ s}^{-1}\text{)}, \tag{4}$$

102 The results of calculations, using the above-described model, will be compared with the predictions of sim-  
103 plified models based on the assumptions that liquid thermal conductivity is infinitely high (Infinite Thermal  
104 Conductivity (ITC) model) and liquid species diffusivity is infinitely fast (Infinite Diffusivity (ID) model) or infi-  
105 nitely slow (Single Component (SI) model).

## 106 4. Results

107 The initial modelling parameters were determined from a set of experimental data of fuel droplets and gas  
108 velocity measured in an optically accessed, direct injection research engine, at part and full load, engine-like  
109 conditions at an engine speed of 1000 rpm. The axial velocity component of the fuel droplets and gas seeding  
110 particles (up to the instance of fuel injection) in the axial direction of the cylinder, at locations along the axis of  
111 the fuel injector, were recorded with respect to time using the Phase and Laser Doppler Anemometry techniques.  
112 The fuel droplet size distributions were measured from the start of fuel injection. The results applicable to the  
113 model were selected for a part load engine case, whereby fuel injection occurred during the late stages of the  
114 compression stroke. The fuel droplet data was ensemble-averaged within the first crank angle interval, immedi-  
115 ately following the start of fuel injection, that contained at least 50 measurement records. The mean diameter of  
116 droplets at the initial stage of evaporation is taken equal to 24  $\mu\text{m}$ , their axial velocity component and initial  
117 temperatures are assumed equal to  $U_{\text{drop}} = 20 \text{ m/s}$  and  $T_d = 296 \text{ K}$ , respectively, air axial velocity component (at  
118 the instance prior to fuel injection) is assumed equal to  $U_{\text{air}} = -4 \text{ m/s}$  (leading to a relative droplet axial velocity

119 component of 24 m/s), ambient air (gas) pressure and temperature are assumed equal to  $p_g = 9$  bar and  $T_g =$   
120 545 K, respectively.

121 The plots of the droplet surface temperatures  $T_s$  and radii  $R_d$  versus time are presented in Fig. 2. Four cases  
122 are shown: (1) the contributions of all 20 components are taken into account using the ETC/ED model (indicated  
123 as (ME)); (2) the contributions of 20 components are taken into account using the ITC/ID model (indicated as  
124 (MI)); (3) the thermodynamic and transport properties of 20 components are averaged to form a single compo-  
125 nent and temperature gradient is ignored (ITC model) (indicated as (SI)); and (4) the ITC model in which gaso-  
126 line fuel is approximated with iso-octane (2,2,4-trimethylpentane; indicated as (IO)) is used.

127 As one can see from Fig. 2, the errors in droplet surface temperatures and evaporation times, predicted by  
128 the SI model are 13.6% and 67.5%, respectively. For the IO model these errors reduce to 6.3% and 47.1%, re-  
129 spectively, and reduce further to 4.8% and 8%, respectively, when the MI model was used. Although the accuracy  
130 of the latter model might be acceptable in some engineering applications, this model cannot describe adequately  
131 the underlying physics of the processes inside droplets (heat conduction and species diffusion) as demonstrated  
132 later in this section. **Note that the approximation of iso-alkanes with n-alkanes, as was done in the previ-  
133 ously developed MDQD model, would lead to a slight decrease in predicted droplet surface temperature  
134 (by up to 1.3%) and slight increase in the evaporation time (by 0.1%).**

135 The same plots as in Fig. 2 but for the cases when 20 components of gasoline fuel are approximated by 15,  
136 11 and 7 QC/C (see Table 3) , using the ETC/ED model are shown in Fig. 3. As can be seen in this figure, the er-  
137 rors in surface temperatures and evaporation times predicted by the model using 15 QC/C are 0.3% and 1.3%,  
138 respectively. These errors increase to 0.5% and 4%, respectively, when gasoline fuel is approximated by 11  
139 QC/C, and further increase to 0.8% and 6.4%, respectively, when gasoline fuel is approximated by 7 QC/C. Even  
140 in the latter case, however, these errors can be tolerated in some practical engineering applications. The accura-  
141 cy of this model is better compared with the accuracy of the MI model, and it describes adequately the underly-  
142 ing physics of the processes in droplets.

143 The same plots as in Fig. 3 but for the cases when 20 components of gasoline fuel are approximated by 6, 5 4  
144 and 3 QC/C (see Table 3), using the ETC/ED model are shown in Figs. 4 and 5. As can be seen in these figures,  
145 the errors in surface temperatures and evaporation times predicted by the model using 6 QC/C are 0.8% and  
146 6.6%, respectively. These errors increase to 2.3% and 9.3%, respectively, when gasoline fuel is approximated by  
147 5 QC/C, and further increase to 2.3% and 9.7%, respectively, when gasoline fuel is approximated by 4 QC/C, and  
148 to 2.4% and 15.8%, respectively, when gasoline fuel is approximated by 3 QC/C. In the latter 3 cases, these errors  
149 are larger than those for the MI model and cannot be tolerated in most engineering applications.

150 The mass fractions of several components, selected out of 20 components, at the surface of the droplet ver-  
151 sus time for the same conditions as in Figs. 2-5, are shown in Fig. 6. As can be seen from this figure, the surface  
152 mass fraction of the heaviest component,  $C_{12}H_{26}$ , increases with time at the expense of the surface mass fractions  
153 of the light components,  $C_5H_{12}$  and  $C_7H_{16}$ , which decrease with time; the mass fractions of intermediate compo-  
154 nents first increase and then decrease with time. This behaviour is similar to the one observed for the compo-  
155 nents in Diesel fuel droplets [13].

156 Mass fractions of n-pentane  $C_5H_{12}$  and propylbenzene  $C_9H_{12}$  versus normalised distance from the centre of  
157 droplet ( $R/R_d$ ) at four time instants, 0.02 ms, 0.3 ms, 0.5 ms and 1 ms are shown in Fig. 7. As can be seen from  
158 this figure, the decrease of mass fraction of n-pentane with time at the surface of the droplet leads to the  
159 generation of n-pentane mass fraction gradient in the body of the droplet. This, in its turn, leads to n-pentane  
160 diffusion from the centre of the droplet to its surface. Similarly, the increase of mass fraction of propylbenzene  
161 with time at the surface of the droplets leads to the generation of propylbenzene negative mass fraction gradient  
162 in the body of the droplet and to propylbenzene diffusion from the surface of the droplet to its centre.

163 The plots of temperatures versus normalised distance from the centre of the droplet at four time instants  
164 are shown in Fig. 8. As one can see from this figure, the effect of temperature gradient due to finite thermal con-  
165 ductivity inside the droplet cannot be ignored, especially at the initial stage of evaporation. This questions the  
166 applicability of the widely used Infinite Thermal Conductivity (ITC) model of droplet heating and evaporation.

167 The predicted values of droplet radii ( $R_d$ ) versus the number of QC/C at four time instants are shown in Fig.  
168 9. As can be seen from this figure, the predictions of the model based on the approximation of gasoline fuel by  
169 6 or more QC/C give reasonably good agreements with the predictions of the model taking into account all 20  
170 components of gasoline fuel.

171 **Note that when the approximation of the 20-components by a smaller number of QC/C is applied, the larger**  
172 **deviation in evaporation time is due in a large part to the very last evaporation period (see Figures 3 and 4) i.e.**  
173 **when droplets have reached sizes of the order of 1-2  $\mu\text{m}$ , while differences are much smaller for droplets of a larger**  
174 **size. Considering that the residual mass for a 1-2  $\mu\text{m}$  drops is practically irrelevant when compared to the total**  
175 **evaporated mass, this observation may further increase the reliability of the chosen approximations.**

176 The plots similar to those shown in Fig. 9, but for droplet surface temperatures, are presented in Fig. 10. As  
177 in the case shown in Fig. 9, we can see from Fig. 10 that the approximations of gasoline fuel by 6 or more QC/C  
178 give reasonably good agreements with the predictions of the model taking into account the contributions of all  
179 20 components of gasoline fuel. These results are compatible with those inferred from the analysis of Figs. 3-5.



180 The CPU efficiencies of the model versus the numbers of QC/C are shown in Fig. 11 (the PC used is an Intel  
181 Xeon (core duo) E8400, 3 GHz and 3 GB RAM). As can be seen from this figure, approximating 20 components of  
182 gasoline fuel by 6 QC/C reduces the required CPU time by more than 70% compared with the model taking into  
183 account the contributions of all 20 components. As can be inferred from the above analysis, choice of 6 QC/C can  
184 ensure a good compromise between CPU efficiency of the model and its accuracy.

## 185 5. Conclusions

186 A new approach to modelling of the heating and evaporation of gasoline fuel droplets in representative con-  
187 ditions for a direct injection internal combustion engine is described. The components with similar molecular  
188 formulae but different molecular structures are replaced with single components, leading to the reduction of the  
189 total number of components used in modelling to 20. As in the previously suggested multi-dimensional quasi-  
190 discrete (MDQD) model, these 20 components of the fuel are replaced with a smaller number of hypothetical  
191 quasi-components and components. Transient diffusion of these quasi-components/components in the liquid  
192 phase, temperature gradient and recirculation inside droplets due to relative velocities between droplets and  
193 ambient air are taken into account.

194 In contrast to the original MDQD model, where n-alkanes and iso-alkanes are merged into one group of al-  
195 kanes, this approach separates the contributions of these two groups. The results are compared with the predic-  
196 tions of several simplified models. In these models, the contributions of 20 components are taken into account  
197 using the infinite thermal conductivity/infinite species diffusivity (ITC/ID) model; the thermodynamic and  
198 transport properties of 20 components are averaged to form a single component and temperature gradient is  
199 ignored (ITC model); and the ITC model in which gasoline fuel is approximated with iso-octane (2,2,4-  
200 trimethylpentane). It is shown that the application of the latter two simplified models leads to under-prediction  
201 of the droplet evaporation time by up to 67% and 47%, respectively, compared to the ones obtained using the  
202 discrete component model taking into account the contributions of 20 components. . The ITC/ID model leads to  
203 under-prediction of this evaporation time by 8%, which can be acceptable in some engineering applications.  
204 This model, however, cannot describe adequately the underlying physics of the processes inside droplets (heat  
205 conduction and species diffusion).

206 It is shown that the approximation of the actual composition of gasoline fuel by 6 quasi-  
207 components/components, using the MDQD model, leads to errors in estimated droplet surface temperatures and  
208 evaporation times of about 0.9% and 6.6% respectively, for the same engine conditions, which can be tolerated  
209 in many practical engineering applications. It is shown that the application of the latter model leads to about

210 70% reduction in CPU time compared to the model taking into account the contributions of all 20 components of  
211 gasoline fuel.

## 212 Acknowledgements

213 The authors are grateful to Ahmed Elwardany and Paul Harris for useful discussions, and INTERREG IVa  
214 (Project E3C3 (4274), Project CEREEV (4224)) and EPSRC (project EP/K020528/1) and the University of Bright-  
215 on for their financial support to the project.

## 216 Appendices

### 217 A. Transport and thermodynamic properties of n-alkanes

#### 218 A.1. Molecular structure, boiling and critical temperatures

219 The chemical formula for n-alkanes is  $C_nH_{2n+2}$ . Using data from [56–58] the dependences of boiling temperature  
220 at atmospheric pressure, critical temperature and pressures on  $n$  were approximated by the following equations,  
221 valid for the range  $4 \leq n \leq 12$ :

$$222 T_b = -1.1328 n^2 + 45.02 n + 111.68 \quad (\text{K}), \quad (5)$$

$$223 T_{cr} = -1.7679 n^2 + 56.967 n + 227.57 \quad (\text{K}), \quad (6)$$

$$224 P_{cr} = -0.0404 n^3 + 1.2475 n^2 - 14.239 n + 79.185 \quad (\text{bar}). \quad (7)$$

225 Regressions in Eqs. (5)-(7) were shown to lead to errors of up to 0.4%, 0.5% and 1.3% respectively.

#### 226 A.2. Liquid density

227 Liquid density was approximated as [56,57]:

$$228 \rho(T) = 1000 A B^{-(1-T_r)^C} \quad (\text{kg m}^{-3}), \quad (8)$$

229 where coefficients  $A$ ,  $B$  and  $C$ , as functions of the carbon number  $n$ , were approximated as (leading to maximum  
230 errors of 0.24%, 0.22% and 2.2% respectively):

$$231 A = -0.000248142613151153 n^2 + 0.00470185738684884 n + 0.213705550811272,$$

$$232 B = 0.0000384180187873567 n^2 - 0.00298658198121256 n + 0.282644927412468, \text{ and}$$

$$233 C = 0.0000635183603757482 n^2 - 0.000196481639624268 n + 0.279692698548249.$$

#### 234 A.3. Liquid viscosity

235 Liquid viscosity was approximated as [56,57]:

$$236 \mu = 10^{(a+\frac{b}{T}+cT+dT^2)-3} \quad (\text{Pa s}^{-1}), \quad (9)$$

237 where the values of coefficients are presented in Table 4.

#### 238 A.4. Liquid heat capacity

239 The temperature dependence of heat capacity, applicable to all groups, is approximated as [59–61]:

$$240 c_p = A_1 + A_2 T + A_3 T^2 \quad (\text{J} \cdot \text{kg}^{-1} \text{K}^{-1}), \quad (10)$$

241 where

$$242 A_1 = 4184 \left( -1.17126 + (0.023722 + 0.024907 \bar{\rho}) K_W + \frac{1.14982 - 0.046535 K_W}{\bar{\rho}} \right),$$

$$243 A_2 = 7531.2 \left( (10^{-4})(1 + 0.82463 K_W) + (1.12172 - \frac{0.27634}{\bar{\rho}}) \right),$$

$$A_3 = 13556.16 \left( (-10^{-8})(1.0 + 0.82463 K_W) + \left( 2.9027 - \frac{0.70958}{\tilde{\rho}} \right) \right),$$

$T_r = T/T_{cr}$  is the reduced temperature,  $T$  is the temperature (in K),  $T_{cr}$  is the critical temperature (in K),  $K_W$  is the Watson characterisation factor, calculated as  $K_W = (1.8 T_b)^{1/3} / \tilde{\rho}$  (see [62]), and  $\tilde{\rho}$  is the relative density at 288.706 K, as shown in Table 5. Approximation (10) is valid for  $0.4 < T_r < 0.85$ .

## 248 A.5. Liquid thermal conductivity

249 Following [1,58,63], the liquid thermal conductivity of  $n$ -alkanes was estimated, using the Latini formula, as:

$$250 \lambda_L = \frac{A(1-T_r)^{0.38}}{(T_r)^6} \quad (\text{W m}^{-1} \text{ K}^{-1}), \quad (11)$$

251 where  $\lambda_L$  is thermal conductivity of liquid,  $A$  is given in the following expression [64]:

$$252 A = \frac{A^* T_b^\alpha}{M_w^\beta T_{cr}^\gamma}, \quad (12)$$

253  $M_w$  is molar mass (in  $\text{g mol}^{-1}$ ); the values of other coefficients are shown in Table 6.

## 254 A.6. Saturated vapour pressure

255 Following [58,65], saturated vapour pressure of  $n$ -alkanes (in Pa) was calculated from the following equation:

$$256 \ln P_r^{\text{vap}} = f^0(T_r) + \omega f^1(T_r), \quad (13)$$

257 where  $f^0$  and  $f^1$  are the Pitzer's functions of  $T_r$ :

$$258 f^0(T_r) = 5.92714 - \frac{6.09648}{T_r} - 1.28862 \ln T_r + 0.169347 \ln T_r^6,$$

$$259 f^1(T_r) = 15.2518 - \frac{15.6875}{T_r} - 13.4721 \ln T_r + 0.43577 \ln T_r^6,$$

$$260 \omega = \frac{-\ln P_{cr} - f^0(\theta)}{f^1(\theta)} \text{ and } \theta = \frac{T_b}{T_{cr}}.$$

261 Eq. (13) is applied to all other groups of components in gasoline fuels.

## 262 A.7. Enthalpy of evaporation

263 Enthalpy of evaporation was estimated using the following expression [56]:

$$264 L = A(1 - T_r)^B \times 10^6 / M_w \quad (\text{J kg}^{-1}), \quad (14)$$

265 where coefficients  $A$  and  $B$  are given in Table 7.

## 266 B. Transport and thermodynamic properties of iso-alkanes

### 267 B.1. Molecular structure, boiling and critical temperatures

268 Using data from [56] the dependence of the boiling temperature at atmospheric pressure, critical temperature  
269 and pressure were approximated by the following expressions, valid for the range  $4 \leq n \leq 11$ :

$$270 T_b = -1.1597 n^2 + 44.011 n + 107.75 \quad (\text{K}), \quad (15)$$

271  $T_{cr} = -2.4511 n^2 + 66.891 n + 183.88$  (K), (16)

272  $P_{cr} = -0.0186 n^3 + 0.459 n^2 - 5.924 n + 54.071$  (bar). (17)

273 Errors of Approximations (17)-(19) were estimated to be 1.45%, 1.61% and 1.17%, respectively.

## 274 B.2. Liquid density

275 The temperature dependence of the liquid density of iso-alkanes was approximated by Expression (8) with coef-  
276 ficients  $A, B$  and  $C$  estimated as [56]:

277  $A = -0.000981411583995317 n^2 + 0.0167403553403262 n + 0.175683060992056,$

278  $B = -0.000706081955526297 n^2 + 0.00873629109926122 n + 0.249117016533684,$  and

279  $C = 0.00114456989247312 n^2 - 0.0174424731182795 n + 0.343958172043011.$

## 280 B.3. Liquid viscosity

281 The liquid viscosity of iso-alkanes was estimated based on Expression (9) with coefficients given in Table 8  
282 [56,57].

## 283 B.4. Liquid heat capacity and thermal conductivity

284 Following [59–61], The liquid heat capacity of iso-alkanes is calculated using Equation (10). Following [1,58,63],  
285 the liquid thermal conductivity of iso-alkanes was estimated using the Latini formula (Equations (11) and (12)).

## 286 B.5. Enthalpy of evaporation and saturated vapour pressure

287 The enthalpy of evaporation was estimated using Equation (14) with coefficients  $A$  and  $B$  given in Table 9. Fol-  
288 lowing [58,65], as in the case on n-alkanes, the saturated vapour pressure of iso-alkanes was calculated from  
289 Equation (13).

## 290 C. Transport and thermodynamic properties of aromatics

### 291 C.1. Molecular structure, boiling and critical temperatures

292 Using data from [56,57], the dependence of boiling temperature at atmospheric pressure, critical temperature  
293 and pressures on  $n$  in the range  $8 \leq n \leq 11$  were approximated as:.

294  $T_b = -1.4662 n^2 + 46.596 n + 136.63$  (K), (18)

295  $T_{cr} = 0.0257 n^2 + 15.718 n + 499.56$  (K), (19)

296  $P_{cr} = 0.7329 n^2 - 17.615 n + 131.36$  (bar). (20)

297 Errors of these approximations were shown to be 2.77%, 3.22% and 0.26% respectively.

## 298 C.2. Liquid density, viscosity, heat capacity and thermal conductivity

299 The liquid density was estimated using Equation (8) with the values of coefficients given in Table 10. The liquid  
300 viscosity was estimated using Equation (9) with the coefficients given in Table 11. Following [59–61], the liquid  
301 heat capacity was calculated using Equation (10). Following [1,58,63], the liquid thermal conductivity was esti-  
302 mated using the Latini formula with the coefficients given in Table 6.

## 303 C.3. Enthalpy of evaporation and saturated vapour pressure

304 The latent heat of evaporation was estimated from Equation (14), using the coefficients given in Table 12. Fol-  
305 lowing [58,65], the saturated vapour pressure of aromatics was calculated from Equation (13) with the critical  
306 pressures given by Equation (19).

## 307 D. Transport and thermodynamic properties of indanes/naphthalenes, cycloalkanes and ole- 308 fins

### 309 D.1. Molecular structure, boiling and critical temperatures

310 The boiling temperature at atmospheric pressure, critical temperature and pressure of characteristic compo-  
311 nents of indanes/naphthalenes ( $C_9H_{10}$ ), cycloalkanes (cis-1-ethyl-3-methylcyclopentane;  $C_8H_{16}$ ), and olefins (1-  
312 nonene;  $C_9H_{18}$ ) are the following [56–58,66]:

313  $T_b = 451.12$  K,  $T_{cr} = 684.9$  K and  $P_{cr} = 39.50$  bar, for indane ( $C_9H_{10}$ );

314  $T_b = 394.25$  K,  $T_{cr} = 586.99$  K and  $P_{cr} = 29.57$  bar, for cis-1-ethyl-3-methylcyclopentane;

315  $T_b = 420.02$  K,  $T_{cr} = 594$  K and  $P_{cr} = 23.30$  bar, for 1-nonene.

### 316 D.2. Liquid density, viscosity, heat capacity and thermal conductivity

317 The liquid densities of the characteristic components for indanes/naphthalenes, cycloalkanes and olefins are  
318 calculated using Equation (8) with the coefficients  $A$ ,  $B$  and  $C$  given in Table 13. The liquid viscosities of the  
319 characteristic components for indanes/naphthalenes, cycloalkanes and olefins were estimated using Expression  
320 (9) with the coefficients given in Table 14. Following [59–61], the liquid heat capacity of the characteristic com-  
321 ponents for indanes/naphthalenes, cycloalkanes and olefins were calculated using Equation (10) with the coeffi-  
322 cients given in Table 5. Following [1,58,63], the liquid thermal conductivities of the characteristic components  
323 for indanes/naphthalenes, cycloalkanes and olefins were estimated using the Latini formula (Equations (11) and  
324 (12)) with the coefficients given in Table 6.

### 325 D.3. Saturated vapour pressure and enthalpy of evaporation

326 Following [58,65], the saturated vapour pressures of the characteristic components for indanes/naphthalenes,  
327 cycloalkanes and olefins were calculated from Equation (13). The latent heats of evaporation of the characteristic  
328 components for indanes/naphthalenes, cycloalkanes and olefins were calculated using Equation (14) with coeffi-  
329 cients *A* and *B* given in Table 15.

### 330 References

- 331 [1] Sawyer RF. Trends in auto emissions and gasoline composition. *Environ Health Perspect* 1993;101:5–12.  
332 [2] Sarathy SM, Kukkadapu G, Mehl M, Wang W, Javed T, Park S, et al. Ignition of alkane-rich FACE gasoline  
333 fuels and their surrogate mixtures. *Proceedings of the Combustion Institute* 2015;35:249–57.  
334 doi:10.1016/j.proci.2014.05.122.  
335 [3] Elwardany AE, Sazhin SS, Farooq A. Modelling of heating and evaporation of gasoline fuel droplets: A com-  
336 parative analysis of approximations. *Fuel* 2013;111:643–7. doi:10.1016/j.fuel.2013.03.030.  
337 [4] Teng ST, Williams AD, Urdal K. Detailed hydrocarbon analysis of gasoline by GC-MS (SI-PIONA). *Journal of*  
338 *High Resolution Chromatography* 1994;17:469–75. doi:10.1002/jhrc.1240170614.  
339 [5] Abramzon B, Sazhin SS. Convective vaporization of a fuel droplet with thermal radiation absorption. *Fuel*  
340 2006;85:32–46. doi:10.1016/j.fuel.2005.02.027.  
341 [6] Sirignano WA. *Fluid Dynamics and Transport of Droplets and Sprays*. Cambridge, U.K: Cambridge Universi-  
342 ty Press; 1999.  
343 [7] Abramzon B, Sazhin S. Droplet vaporization model in the presence of thermal radiation. *International Jour-*  
344 *nal of Heat and Mass Transfer* 2005;48:1868–73. doi:10.1016/j.ijheatmasstransfer.2004.11.017.  
345 [8] Elwardany AE, Sazhin SS. A quasi-discrete model for droplet heating and evaporation: Application to Diesel  
346 and gasoline fuels. *Fuel* 2012;97:685–94. doi:10.1016/j.fuel.2012.01.068.  
347 [9] Elwardany AE, Gusev IG, Castanet G, Lemoine F, Sazhin SS. Mono- and multi-component droplet cool-  
348 ing/heating and evaporation: comparative analysis of numerical models. *Atomization and Sprays*  
349 2011;21:907–31. doi:10.1615/AtomizSpr.2012004194.  
350 [10] Sazhin SS. Advanced models of fuel droplet heating and evaporation. *Progress in Energy and Combustion*  
351 *Science* 2006;32:162–214. doi:10.1016/j.pecs.2005.11.001.  
352 [11] Sazhin SS, Al Qubeissi M, Kolodnytska R, Elwardany AE, Nasiri R, Heikal MR. Modelling of biodiesel fuel  
353 droplet heating and evaporation. *Fuel* 2014;115:559–72. doi:10.1016/j.fuel.2013.07.031.  
354 [12] Sazhin SS, Elwardany AE, Sazhina EM, Heikal MR. A quasi-discrete model for heating and evaporation of  
355 complex multicomponent hydrocarbon fuel droplets. *International Journal of Heat and Mass Transfer*  
356 2011;54:4325–32. doi:10.1016/j.ijheatmasstransfer.2011.05.012.  
357 [13] Sazhin SS, Al Qubeissi M, Nasiri R, Gun'ko VM, Elwardany AE, Lemoine F, et al. A multi-dimensional quasi-  
358 discrete model for the analysis of Diesel fuel droplet heating and evaporation. *Fuel* 2014;129:238–66.  
359 doi:10.1016/j.fuel.2014.03.028.  
360 [14] Sazhin SS, Shishkova IN, Al Qubeissi M. Heating and evaporation of a two-component droplet: Hydrody-  
361 namic and kinetic models. *International Journal of Heat and Mass Transfer* 2014;79:704–12.  
362 doi:10.1016/j.ijheatmasstransfer.2014.08.026.  
363 [15] Sazhin SS, Al Qubeissi M, Xie J-F. Two approaches to modelling the heating of evaporating droplets. *Interna-*  
364 *tional Communications in Heat and Mass Transfer* 2014;57:353–6.  
365 doi:10.1016/j.icheatmasstransfer.2014.08.004.  
366 [16] Sazhin SS. *Droplets and Sprays*. London: Springer; 2014.  
367 [17] Ma X, Jiang C, Xu H, Ding H, Shuai S. Laminar burning characteristics of 2-methylfuran and isooctane blend  
368 fuels. *Fuel* 2014;116:281–91. doi:10.1016/j.fuel.2013.08.018.  
369 [18] Paxson FL. *The Last American Frontier*. Simon Publications LLC; 2001.  
370 [19] Sazhin SS, Kristyadi T, Abdelghaffar WA, Begg S, Heikal MR, Mikhalovsky SV, et al. Approximate Analysis of  
371 Thermal Radiation Absorption in Fuel Droplets. *Journal of Heat Transfer* 2007;129:1246.  
372 doi:10.1115/1.2740304.  
373 [20] Pitz WJ, Cernansky NP, Dryer FL, Egolfopoulos FN, Farrell JT, Friend DG, et al. Development of an Experi-  
374 mental Database and Chemical Kinetic Models for Surrogate Gasoline Fuels. Warrendale, PA: SAE Interna-  
375 tional; 2007.  
376 [21] Abraham J, Magi V. *A Model for Multicomponent Droplet Vaporization in Sprays*. Warrendale, PA: SAE In-  
377 ternational; 1998.

- 378 [22] Aggarwal SK, Mongia HC. Multicomponent and High-Pressure Effects on Droplet Vaporization. *Journal of*  
379 *Engineering for Gas Turbines and Power* 2002;124:248. doi:10.1115/1.1423640.
- 380 [23] Continillo G, Sirignano WA. Unsteady, Spherically-Symmetric Flame Propagation Through Multicomponent  
381 Fuel Spray Clouds. In: Angelino G, Luca LD, Sirignano WA, editors. *Modern Research Topics in Aerospace*  
382 *Propulsion*, Springer New York; 1991, p. 173–98.
- 383 [24] Klingsporn M, Renz U. Vaporization of a binary unsteady spray at high temperature and high pressure. *Inter-*  
384 *national Journal of Heat and Mass Transfer* 1994;37:265–72. doi:10.1016/0017-9310(94)90027-2.
- 385 [25] Lage PLC, Hackenberg CM, Rangel RH. Nonideal vaporization of dilating binary droplets with radiation ab-  
386 sorption. *Combustion and Flame* 1995;101:36–44. doi:10.1016/0010-2180(94)00191-T.
- 387 [26] Maqua C, Castanet G, Lemoine F. Bicomponent droplets evaporation: Temperature measurements and  
388 modelling. *Fuel* 2008;87:2932–42. doi:10.1016/j.fuel.2008.04.021.
- 389 [27] Ra Y, Reitz RD. A vaporization model for discrete multi-component fuel sprays. *International Journal of*  
390 *Multiphase Flow* 2009;35:101–17. doi:10.1016/j.ijmultiphaseflow.2008.10.006.
- 391 [28] Tong AY, Sirignano WA. Multicomponent Transient Droplet Vaporization with Internal Circulation: Integral  
392 Equation Formulation and Approximate Solution. *Numerical Heat Transfer* 1986;10:253–78.  
393 doi:10.1080/10407788608913519.
- 394 [29] Abdel-Qader Z, Hallett WLH. The role of liquid mixing in evaporation of complex multicomponent mix-  
395 tures: modelling using continuous thermodynamics. *Chemical Engineering Science* 2005;60:1629–40.  
396 doi:10.1016/j.ces.2004.10.015.
- 397 [30] Arias-Zugasti M, Rosner DE. Multicomponent fuel droplet vaporization and combustion using spectral the-  
398 ory for a continuous mixture. *Combustion and Flame* 2003;135:271–84. doi:10.1016/S0010-  
399 2180(03)00166-4.
- 400 [31] Hallett WLH. A simple model for the vaporization of droplets with large numbers of components. *Combust-*  
401 *ion and Flame* 2000;121:334–44. doi:10.1016/S0010-2180(99)00144-3.
- 402 [32] Lippert AM, Reitz RD. Modeling of multicomponent fuels using continuous distributions with application to  
403 droplet evaporation and sprays. Warrendale, PA: SAE International; 1997.
- 404 [33] Rivard E, Brüggemann D. Numerical investigation of semi-continuous mixture droplet vaporization at low  
405 temperature. *Chemical Engineering Science* 2010;65:5137–45. doi:10.1016/j.ces.2010.06.010.
- 406 [34] Tamim J, Hallett WLH. A continuous thermodynamics model for multicomponent droplet vaporization.  
407 *Chemical Engineering Science* 1995;50:2933–42. doi:10.1016/0009-2509(95)00131-N.
- 408 [35] Zhang L, Kong S-C. Modeling of multi-component fuel vaporization and combustion for gasoline and diesel  
409 spray. *Chemical Engineering Science* 2009;64:3688–96. doi:10.1016/j.ces.2009.05.013.
- 410 [36] Zhu G-S, Reitz RD. A model for high-pressure vaporization of droplets of complex liquid mixtures using  
411 continuous thermodynamics. *International Journal of Heat and Mass Transfer* 2002;45:495–507.  
412 doi:10.1016/S0017-9310(01)00173-9.
- 413 [37] Burger M, Schmehl R, Prommersberger K, Schäfer O, Koch R, Wittig S. Droplet evaporation modeling by the  
414 distillation curve model: accounting for kerosene fuel and elevated pressures. *International Journal of Heat*  
415 *and Mass Transfer* 2003;46:4403–12. doi:10.1016/S0017-9310(03)00286-2.
- 416 [38] Ott LS, Smith BL, Bruno TJ. Composition-Explicit Distillation Curves of Waste Lubricant Oils and Resourced  
417 Crude Oil: A Diagnostic for Re-Refining and Evaluation. *American Journal of Environmental Sciences*  
418 2010;6:523–34. doi:10.3844/ajessp.2010.523.534.
- 419 [39] Smith BL, Bruno TJ. Advanced Distillation Curve Measurement with a Model Predictive Temperature Con-  
420 troller. *Int J Thermophys* 2006;27:1419–34. doi:10.1007/s10765-006-0113-7.
- 421 [40] Al Qubeissi M, Kolodnytska R, Sazhin SS. Biodiesel fuel droplets: modelling of heating and evaporation pro-  
422 cesses. 25th European Conference on Liquid Atomization and Spray Systems, vol. 4 (CD), Crete, Greece:  
423 2013.
- 424 [41] Elwardany AE. Modelling of multi-component fuel droplets heating and evaporation. PhD thesis. University  
425 of Brighton, 2012.
- 426 [42] Laurent C, Lavergne G, Villedieu P. Continuous thermodynamics for droplet vaporization: Comparison be-  
427 tween Gamma-PDF model and QMoM. *Comptes Rendus Mécanique* 2009;337:449–57.  
428 doi:10.1016/j.crme.2009.06.004.
- 429 [43] Zhang L, Kong S-C. Vaporization modeling of petroleum-biofuel drops using a hybrid multi-component  
430 approach. *Combustion and Flame* 2010;157:2165–74. doi:10.1016/j.combustflame.2010.05.011.
- 431 [44] Zhang L. Multicomponent drop vaporization modeling of petroleum and biofuel mixtures. Iowa State Uni-  
432 versity, 2011.
- 433 [45] Tonini S, Gavaises M, Arcoumanis C, Theodorakakos A, Kometani S. Multi-component fuel vaporization  
434 modelling and its effect on spray development in gasoline direct injection engines. *Proceedings of the Insti-*  
435 *tution of Mechanical Engineers, Part D: Journal of Automobile Engineering* 2007;221:1321–42.  
436 doi:10.1243/09544070JAUTO545.
- 437 [46] Strotos G, Gavaises M, Theodorakakos A, Bergeles G. Numerical investigation of the evaporation of two-  
438 component droplets. *Fuel* 2011;90:1492–507. doi:10.1016/j.fuel.2011.01.017.



- 439 [47] Al Qubeissi M, Sazhin SS, de Sercey G, Crua C. Multi-dimensional quasi-discrete model for the investigation  
440 of heating and evaporation of Diesel fuel droplets. 26th European Conference on Liquid Atomization and  
441 Spray Systems, vol. ABS-135 (CD), Bremen, Germany: University of Bremen; 2014.
- 442 [48] Abramzon B, Sirignano WA. Droplet vaporization model for spray combustion calculations. *International*  
443 *Journal of Heat and Mass Transfer* 1989;32:1605–18. doi:10.1016/0017-9310(89)90043-4.
- 444 [49] Al Qubeissi M, Sazhin SS, Crua C, Heikal MR. Modelling of Heating and Evaporation of Biodiesel Fuel Drop-  
445 lets. *WASET, Int J Mech Aero Ind Mechat Eng* 2015;9:46–9.
- 446 [50] Sazhin SS, Elwardany AE, Krutitskii PA, Deprédurand V, Castanet G, Lemoine F, et al. Multi-component  
447 droplet heating and evaporation: Numerical simulation versus experimental data. *International Journal of*  
448 *Thermal Sciences* 2011;50:1164–80. doi:10.1016/j.ijthermalsci.2011.02.020.
- 449 [51] Sazhin SS, Abdelghaffar WA, Krutitskii PA, Sazhina EM, Heikal MR. New approaches to numerical modelling  
450 of droplet transient heating and evaporation. *International Journal of Heat and Mass Transfer*  
451 2005;48:4215–28. doi:10.1016/j.ijheatmasstransfer.2005.04.007.
- 452 [52] Sazhin SS, Kristyadi T, Abdelghaffar WA, Heikal MR. Models for fuel droplet heating and evaporation: Com-  
453 parative analysis. *Fuel* 2006;85:1613–30. doi:10.1016/j.fuel.2006.02.012.
- 454 [53] Tonini S, Cossali GE. An analytical model of liquid drop evaporation in gaseous environment. *International*  
455 *Journal of Thermal Sciences* 2012;57:45–53. doi:10.1016/j.ijthermalsci.2012.01.017.
- 456 [54] Rogers MC, Brown GG. Raoult's Law and the Equilibrium Vaporization of Hydrocarbon Mixtures. University  
457 of Michigan; 1929.
- 458 [55] Sazhin SS, Elwardany A, Krutitskii PA, Castanet G, Lemoine F, Sazhina EM, et al. A simplified model for bi-  
459 component droplet heating and evaporation. *International Journal of Heat and Mass Transfer*  
460 2010;53:4495–505. doi:10.1016/j.ijheatmasstransfer.2010.06.044.
- 461 [56] Yaws CL. *Thermophysical Properties of Chemicals and Hydrocarbons*. Norwich, NY: William Andrew; 2008.
- 462 [57] Yaws CL. *Thermophysical properties of chemicals and hydrocarbons*. 2nd ed. Oxford, UK: 2014.
- 463 [58] Poling BE, Prausnitz JM, O'Connell JP. *The Properties of Gases and Liquids*. New York: McGraw-Hill; 2001.
- 464 [59] Dadgostar N, Shaw JM. A predictive correlation for the constant-pressure specific heat capacity of pure and  
465 ill-defined liquid hydrocarbons. *Fluid Phase Equilibria* 2012;313:211–26. doi:10.1016/j.fluid.2011.09.015.
- 466 [60] Lee BI, Kesler MG. Private Communication. Princeton, N.J.: Mobil Oil Corporation; 1975.
- 467 [61] Lee BI, Kesler MG. A generalized thermodynamic correlation based on three-parameter corresponding  
468 states. *AIChE J* 1975;21:510–27. doi:10.1002/aic.690210313.
- 469 [62] Gharagheizi F, Fazeli A. Prediction of the Watson Characterization Factor of Hydrocarbon Components  
470 from Molecular Properties. *QSAR Comb Sci* 2008;27:758–67. doi:10.1002/qsar.200730020.
- 471 [63] Latini G, Cocci Grifoni R, Passerini G, editors. *Transport properties of organic liquids*. Southampton ; Bos-  
472 ton: WIT Press; 2006.
- 473 [64] Latini G, Cocci Grifoni R, Passerini G, editors. *Transport Properties of Organic Liquids*. Southampton ; Bos-  
474 ton: WIT Press; 2006.
- 475 [65] Komkoua Mbienda AJ, Tchawoua C, Vondou DA, Mkankam Kamga F. Evaluation of Vapor Pressure Estima-  
476 tion Methods for Use in Simulating the Dynamic of Atmospheric Organic Aerosols. *International Journal of*  
477 *Geophysics* 2013;2013:e612375. doi:10.1155/2013/612375.
- 478 [66] Yaws CL. *The Yaws handbook of vapor pressure: Antoine coefficients*. Houston, Tex.: Gulf Pub.; 2007.
- 479 [67] ChemSpider 2014. <http://www.chemspider.com/> (accessed December 30, 2014).
- 480

## 481 Figure captions

482 Fig. 1 The structures of some organic components of gasoline fuel, generated using software [67].

483 Fig. 2 The droplet surface temperatures  $T_s$  and radii  $R_d$  versus time for the cases when 1) the contributions of all  
484 20 components are taken into account using the ETC/ED model (ME); 2) the contribution of 20 components are  
485 taken into account using the ITC/ID model (MI), 3) the 20 component are approximated by a single component  
486 with average thermodynamic and transport properties in combination with the ITC model (SI); 4) gasoline fuel  
487 is approximated by iso-octane in combination with the ITC model (IO). The droplet with the initial radius 12  $\mu\text{m}$   
488 and initial homogeneous temperature 296 K is assumed to be moving with relative velocity 24 m/s in air. Ambi-  
489 ent pressure and temperature are equal to 0.9 MPa and 545 K respectively.

490 Fig. 3 The same as Fig. 2 but for the cases when the ETC/ED model was used taking into account the contribu-  
491 tions of all 20 components of gasoline fuel (indicated as ME) and assuming that these components are  
492 approximated by 15, 11 and 7 quasi-components/components (QC/C) (numbers are indicated near the plots).

493 Fig. 4 The same as Fig. 3 but for the cases when 20 components of gasoline fuel are approximated by 6, 5, 4 and 3  
494 quasi-components/components (QC/C).

495 Fig. 5 The zoomed parts of Fig. 4.

496 Fig. 6 The surface mass fractions  $Y_{i,s}$  versus time for  $C_5H_{12}$  (1),  $C_{12}H_{26}$  (2), iso -  $C_7H_{16}$  (3), iso -  $C_8H_{18}$  (4),  
497 iso -  $C_{10}H_{22}$  (5),  $C_9H_{12}$  (6),  $C_{10}H_{14}$  (7) and indane  $C_9H_{10}$  (approximation for indanes/naphthenes) (8),  
498 predicted by the ETC/ED model taking into account the contributions of all 20 components of gasoline fuel.

499 Fig. 7 Mass fractions of n-pentane  $C_5H_{12}$  (N) and propylbenzene  $C_9H_{12}$  (P) versus normalised distance from the  
500 centre of droplet ( $R/R_d$ ) at four time instants, 0.02 ms, 0.3 ms, 0.5 ms and 1 ms (indicated near the plots), pre-  
501 dicted by the ETC/ED model taking into account the contributions of all 20 components of gasoline fuel.

502 Fig. 8 The plots of temperature versus normalised distance from the droplet centre ( $R/R_d$ ) at three instants of  
503 time 0.02 ms, 0.3 ms and 0.5 ms (indicated near the plots) as predicted by the ETC/ED model, taking into  
504 account the contributions of all 20 components.

505 Fig. 9 The droplet radii versus the number of QC/C, used for the approximation of gasoline fuel, at four time  
506 instants, 0.5 ms, 1.5 ms, 3 ms, and 4 ms.

507 Fig. 10 The droplet surface temperatures versus the number of QC/C, used for the approximation of gasoline fuel,  
508 at four time instants, 0.5 ms, 1.5 ms, 3 ms, and 4 ms.

509 Fig. 11 Plot of CPU time required for calculations of droplet heating and evaporation versus the number of QC/C  
510 used in the model for the same input parameters as in Figs. 2-10.

## 511 Table captions

512 Table 1 The original and simplified compositions of gasoline fuel used in the analysis.

513 Table 2 The groups of component of gasoline fuel, their molar fractions, and the numbers of components in the  
514 groups, as inferred from Table 1.

515 **Table 3 Numbers of QC/C in various groups of components for several total numbers of QC/C.**

516 Table 4 The coefficients used in Equation (8) for estimating the liquid viscosity of n-alkanes.

517 Table 5 The carbon numbers and relative densities of components at 288.706 K.

518 Table 6 The coefficients used in Equation (11) for six groups of components.

519 Table 7 The coefficients used in Equation (16) for estimation of the enthalpy of evaporation of iso-alkanes.

520 Table 8 The coefficients used in Equation (8) for estimating the liquid viscosity of iso-alkanes

521 Table 9 The coefficients used in Equation (16) for estimating the enthalpy of evaporation of iso-alkanes.

522 Table 10 The coefficients used in Equation (7) for the estimation of the liquid density of aromatics.

523 Table 11 The coefficients used in Equation (8) for estimating the liquid viscosity of aromatics.

524 Table 12 The coefficients used in Equation (16) for estimation of the enthalpy of evaporation of aromatics.

525 Table 13 The coefficients used in Equation (7) for the estimation of the liquid density of three characteristic

526 components for indanes/naphthalenes, cycloalkanes and olefins.

527 Table 14 The coefficients used in Equation (8) for estimating the liquid viscosity of the characteristic compo-

528 nents for indanes/naphthalenes, cycloalkanes and olefins.

529 Table 15 The coefficients used in Equation (16) for estimation of the enthalpy of evaporation of three character-

530 istic components for indanes/naphthalenes, cycloalkanes and olefins.

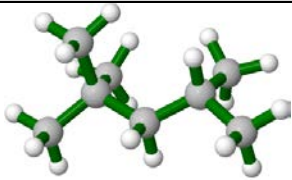
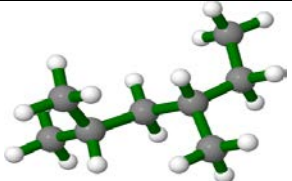
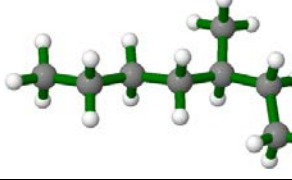
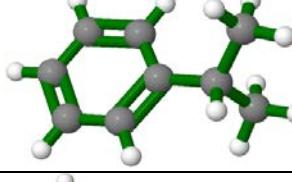
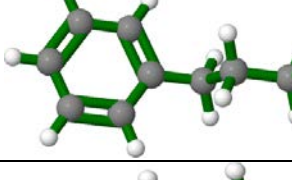
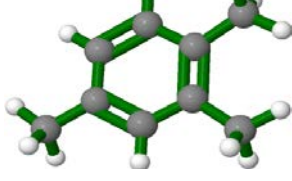
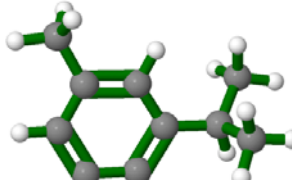
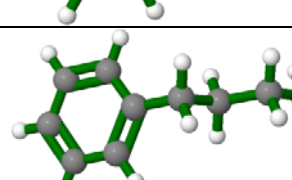
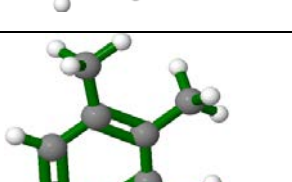
component	Structure	Shape
iso-octane (C <sub>8</sub> H <sub>18</sub> )	2,2,4-trimethylpentane	
	2,4-dimethylhexane	
	3-methylheptane	
C <sub>9</sub> H <sub>12</sub>	i-propylbenzene,	
	n-propylbenzene	
	1,2,4-trimethylbenzene	
C <sub>10</sub> H <sub>14</sub>	3-isopropyl-1-methylbenzene	
	n-butylbenzene	
	3-ethyl-1,2-dimethylbenzene	

Fig. 1

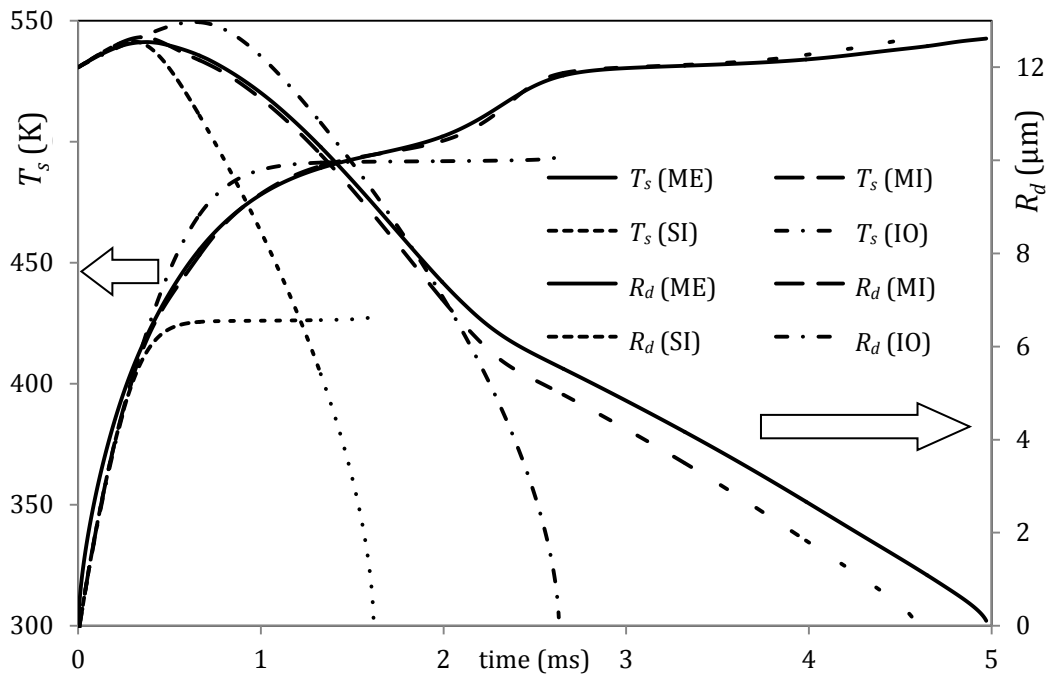


Fig. 2

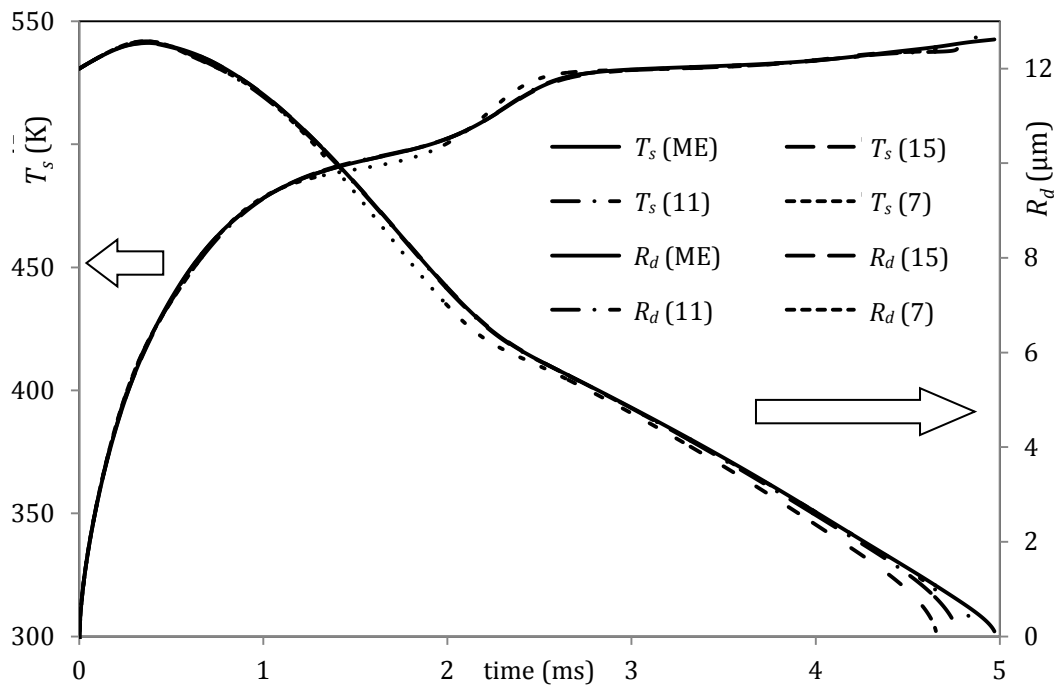


Fig. 3

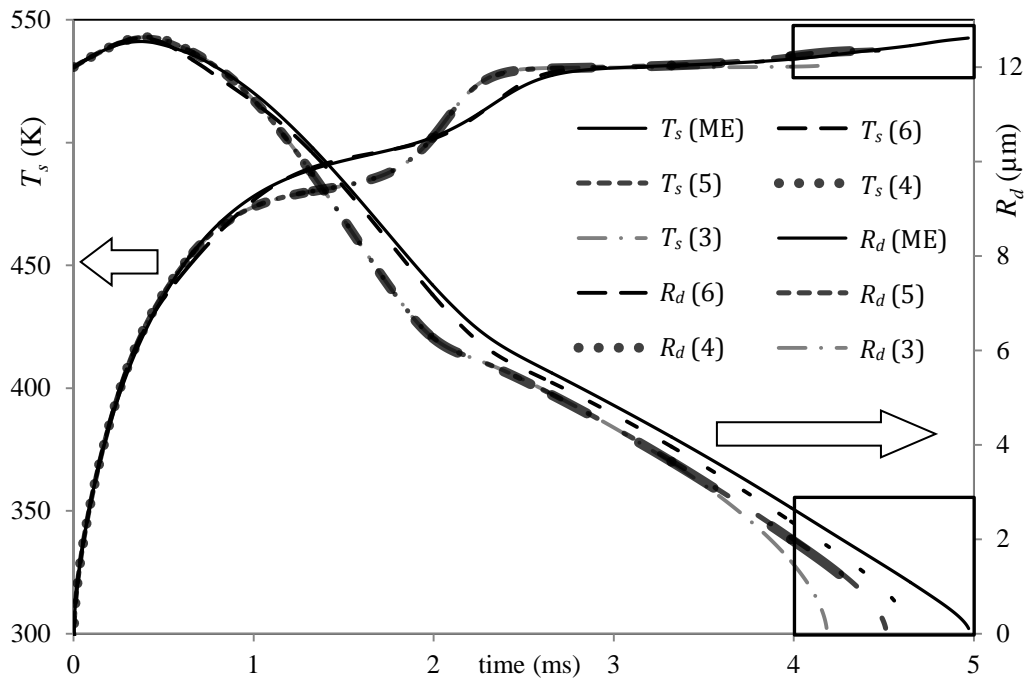


Fig. 4

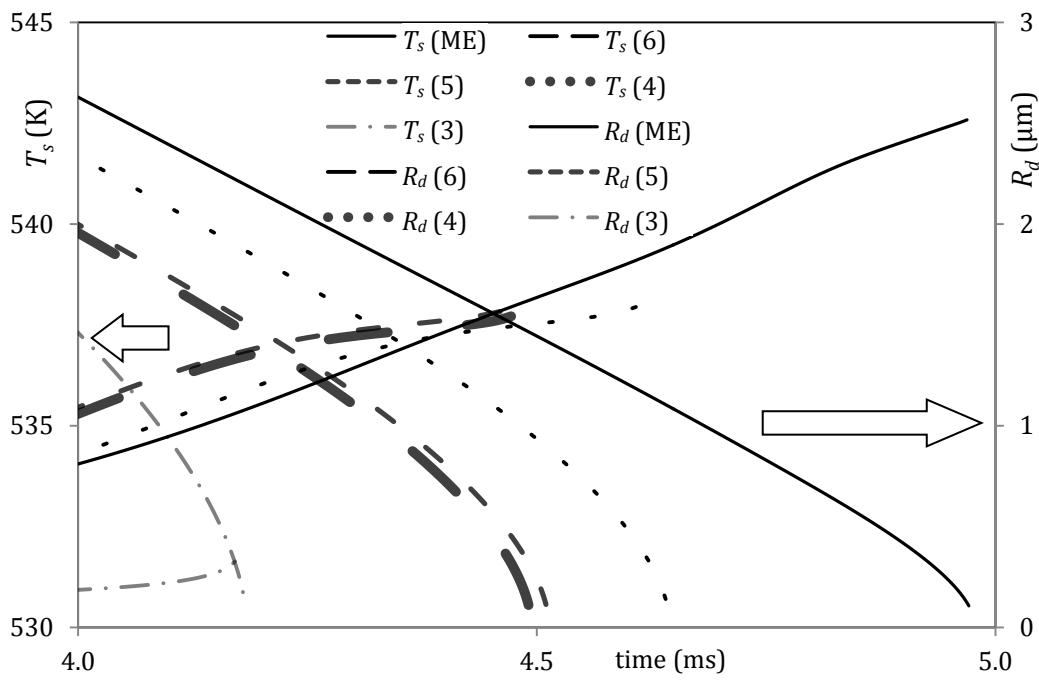


Fig. 5

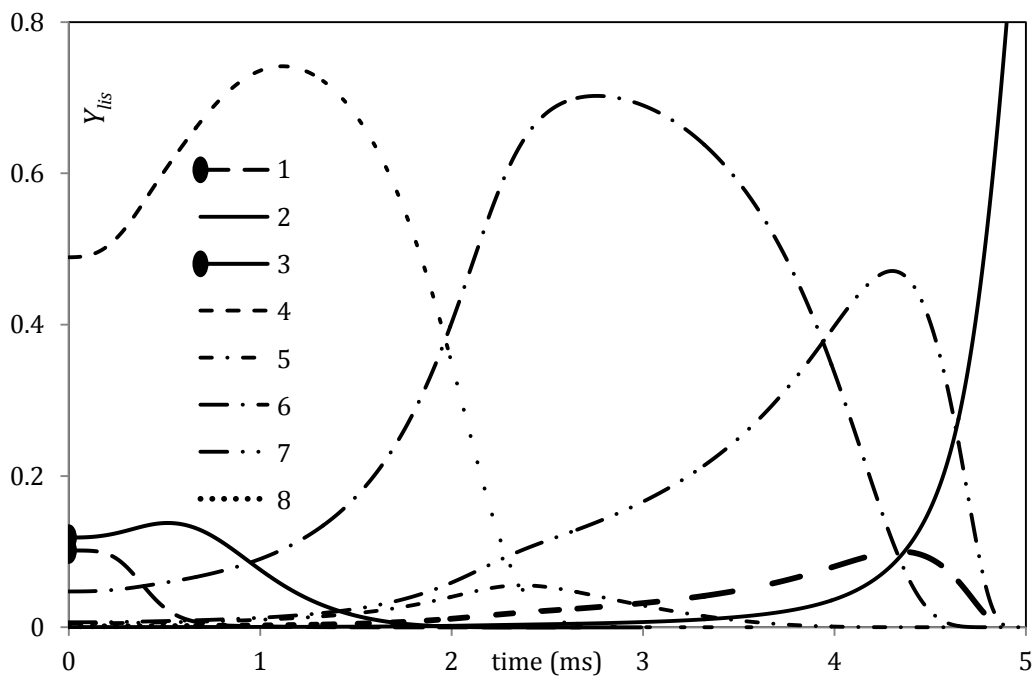


Fig. 6

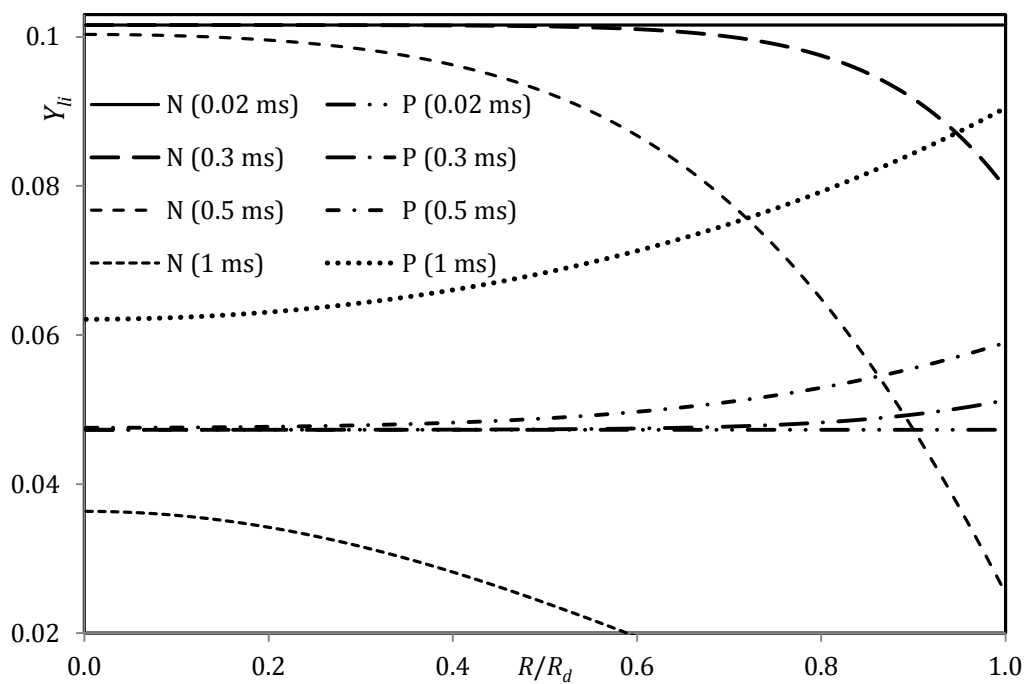


Fig. 7

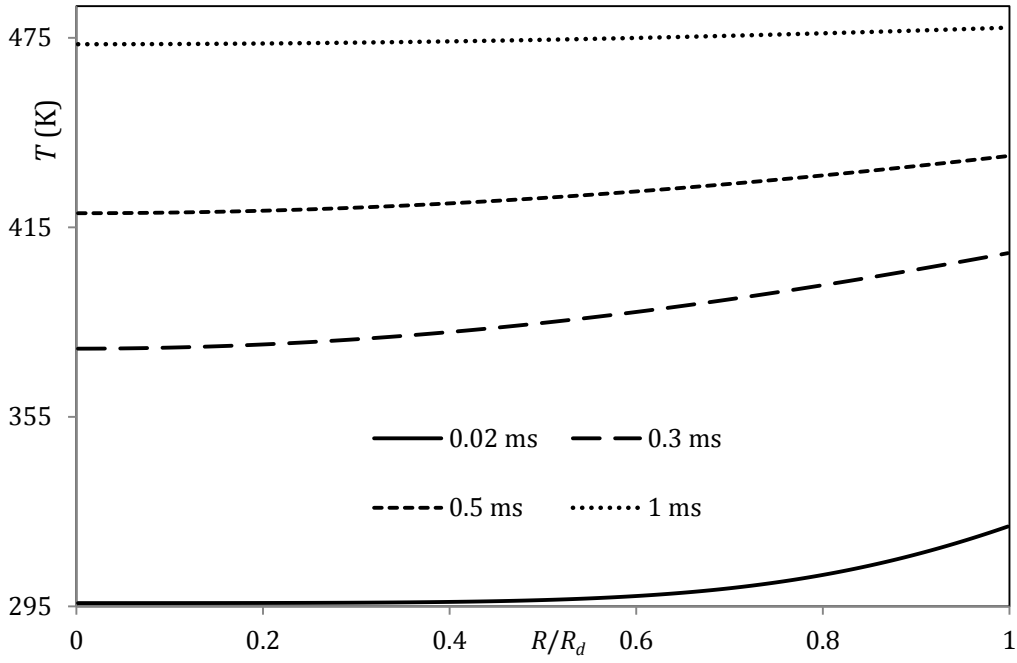


Fig. 8

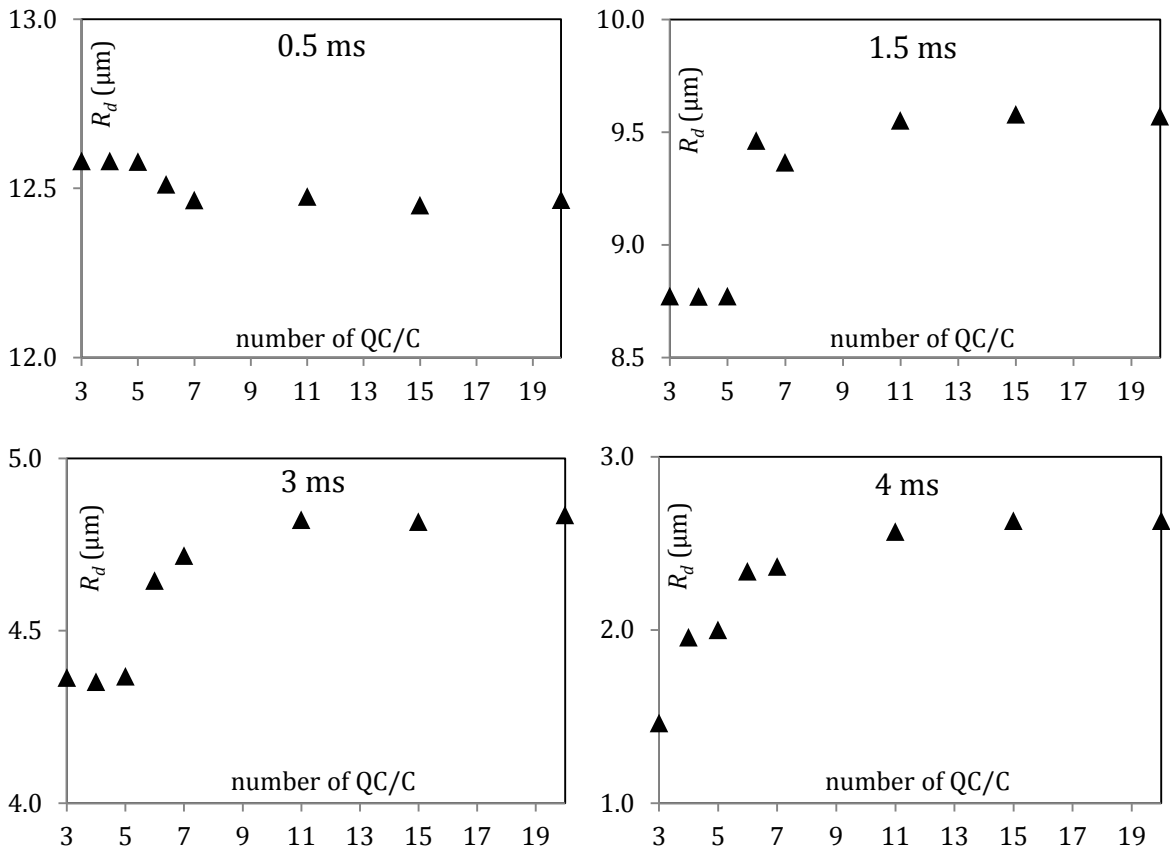


Fig. 9



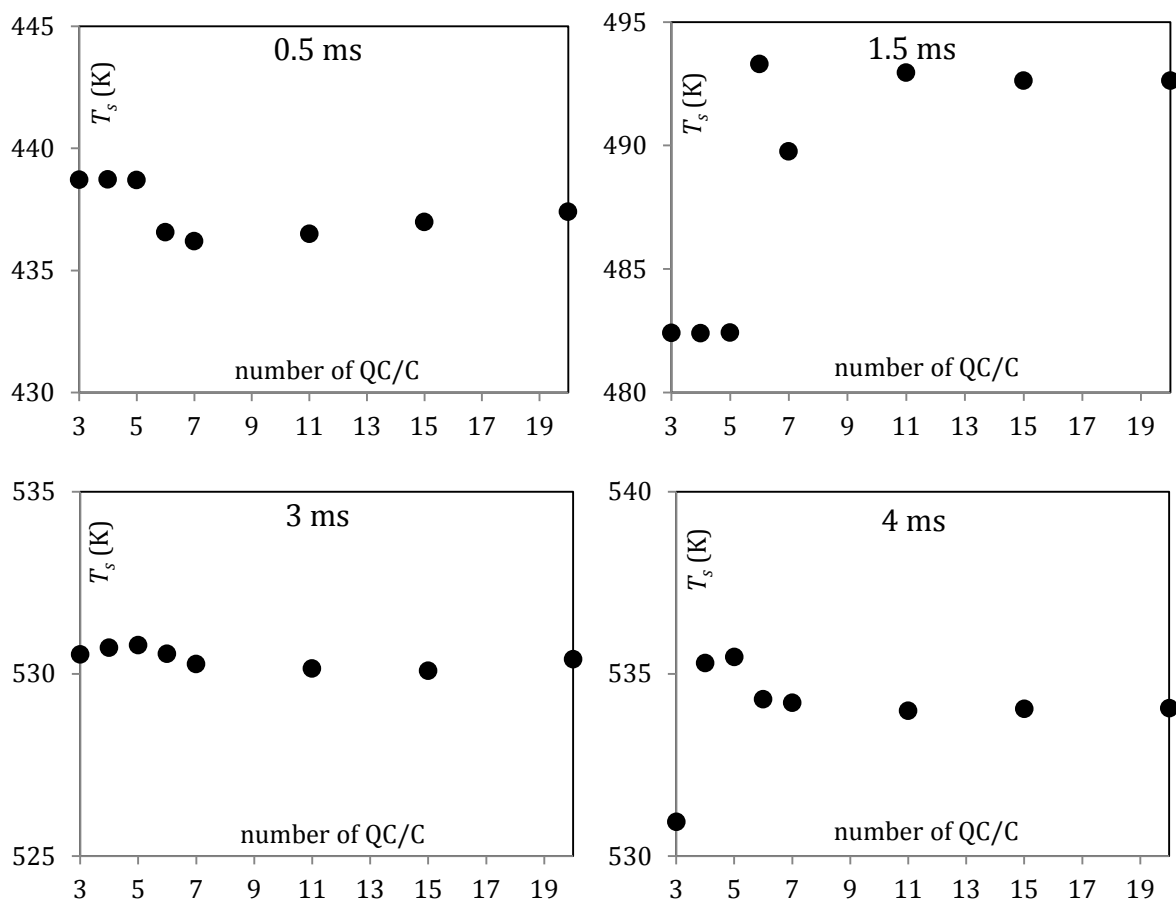


Fig. 10

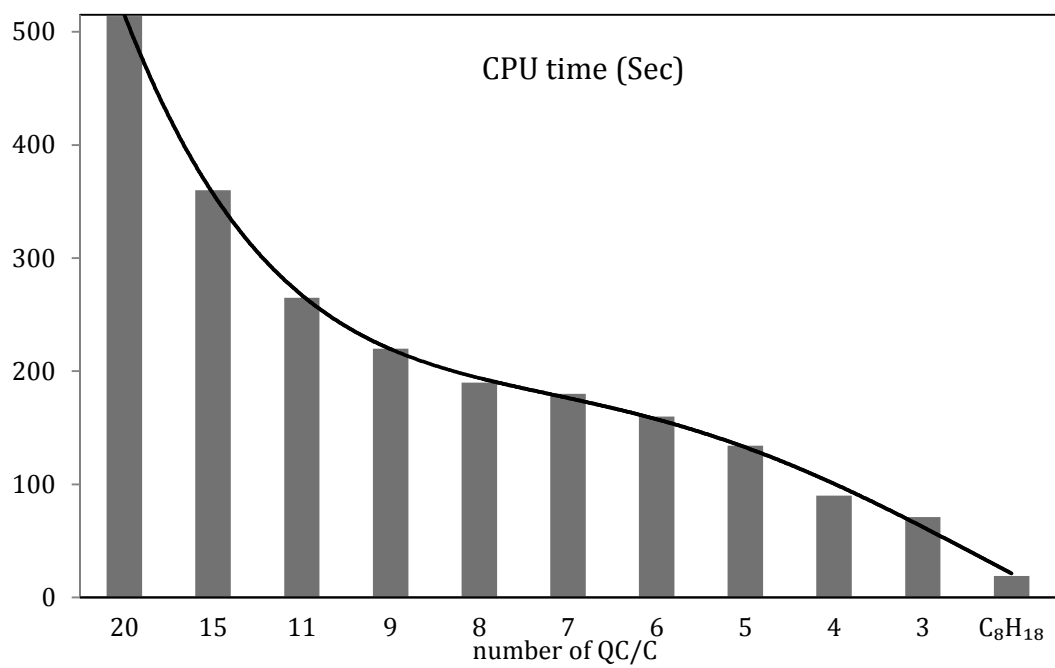


Fig. 11

Table 1

group	components	carbon numbers	molar fractions (%)	approximations	molar fractions (%)
n-alkanes	n-butane	4	3.905436784	same	3.905436784
	n-pentane	5	13.87020578	same	13.87020578
	n-hexane	6	10.84154056	same	10.84154056
	n-decane	10	0.010008808	same	0.010008808
	n-dodecane	12	0.012010569	same	0.012010569
iso-alkanes	i-butane	4	0.092081031	same	0.092081031
	2,2-dimethylpropane i-pentane	5 5	0.012010569 7.444551205	averaged	7.456561774
	2,3-dimethylbutane 2-methylpentane 3-methylpentane	6 6 6	2.021779166 0.604531988 0.353310914	averaged	2.979622067
	2,4-dimethylpentane 2,2,3-trimethylbutane 2-methylhexane 2,3,-dimethylpentane 3-methylhexane	7 7 7 7 7	4.271759148 0.044038754 0.253222836 6.883057090 0.216190247	averaged	11.66826808
	2,2,4-trimethylpentane 2,5-dimethylhexane 2,2,3-trimethylpentane 2,4-dimethylhexane 2,3,4-trimethylpentane 2,3,3-trimethylpentane 2,3-dimethylhexane 2-methyl-3-ethylpentane 2-methylheptane 4-methylheptane 3-methyl-3-ethylpentane 3,4-dimethylhexane 3-methylheptane	8 8 8 8 8 8 8 8 8 8 8 8 8 8	23.23644807 1.739530787 0.550484426 2.369084795 6.905076467 4.947353671 1.888662023 0.068059893 0.060052847 0.021018496 0.152133878 0.175154136 0.060052847	averaged	42.17311234
	2,3,4-trimethylhexane 2,2,3-trimethylhexane 2,5-dimethylheptane 2,3,-dimethylheptane	9 9 9 9	0.179157659 0.02602290 0.069060773 0.043037873	averaged	0.317279206
	c10 - isoparaffin-1 c10 - isoparaffin-2 3,3,5-trimethylheptane 2,3,6-trimethylheptane c10 - isoparaffin-1 2,6-dimethyloctane c10 - isoparaffin-7	10 10 10 10 10 10 10	0.025022019 0.128112739 0.096084554 0.05204580 0.016014092 0.029025542 0.014012331	averaged	0.360317079
	2,3,3,trimethyloctane 2,5-dimethylnonane 3-ethylnonane	11 11 11	0.012010569 0.081071343 0.020017616	averaged	0.113099528
	o-xylene	8	0.242213148	same	0.242213148

group	components	carbon numbers	molar fractions (%)	approximations	molar fractions (%)
aromatics	i-propylbenzene	9	0.046040516	averaged	3.521098567
	n-propylbenzene	9	0.172151493		
	3-ethyl-1-methylbenzene	9	0.621546961		
	4-ethyl-1-methylbenzene	9	0.287252782		
	1,3,5-trimethylbenzene	9	0.383337337		
	2-ethyl-1-methylbenzene	9	0.462406918		
	1,2,4-trimethylbenzene	9	1.304147650		
	1,2,3-trimethylbenzene	9	0.244214909		
	sec-butylbenzene	10	0.012010569	averaged	0.440387541
	3-isopropyl-1-methylbenzene	10	0.033029066		
	4-isopropyl-1-methylbenzene	10	0.009007927		
	1,3-diethylbenzene	10	0.030026423		
	3-propyl-1-methylbenzene	10	0.080070462		
	4-propyl-1-methylbenzene	10	0.035030827		
	n-butylbenzene	10	0.016014092		
	5-ethyl-1,3-dimethylbenzene	10	0.059051966		
	2-propyl-1-methylbenzene	10	0.021018496		
	2-ethyl-1,4-dimethylbenzene	10	0.038033469		
4-ethyl-1,3-dimethylbenzene	10	0.033029066			
4-ethyl-1,2-dimethylbenzene	10	0.059051966			
3-ethyl-1,2-dimethylbenzene	10	0.015013212			
4-isopropyl-1-ethylbenzene	11	0.023020258	averaged	0.055048443	
1-butyl-1-methylbenzene	11	0.032028185			
indanes/ naphthalenes	5-methylindan	10	0.010008808	indane (C <sub>9</sub> H <sub>10</sub> )	0.104091601
	2-methylindan	10	0.009007927		
	naphthalene	10	0.019016735		
	indane (indenes)	9	0.066058131		
cycloalkanes	3c-ethylmethylcyclopentane	8	1.345183762	3c-ethylmethylcyclopentane (C <sub>8</sub> H <sub>16</sub> )	1.491312355
	1,1,methylethylcyclopentane	8	0.022019377		
	c8 - mononaph - 3	8	0.060052847		
	methylcycloheptane	8	0.046040516		
	1-methyl-2-propylcyclohexane	10	0.018015854		
olefins	1-pentene	5	0.046040516	1-nonene (C <sub>9</sub> H <sub>18</sub> )	0.346304748
	c-pentene-2	5	0.016014092		
	1-hexene	6	0.007006165		
	1-nonene	9	0.195171751		
	(z) 2-decene	10	0.056049323		
	3-ethyl-2-methyl-2-heptene	10	0.013011450		
	c-10-isoolefin-9	10	0.013011450		

Table 2

<i>m</i>	group	molar fractions (%)	number of components
1	n-alkanes	28.50	5
2	iso-alkanes	65.18	8
3	aromatics	4.40	4
4	indanes/naphthalenes	0.10	1
5	cycloalkanes	0.33	1
6	olefins	1.49	1

Table 3

groups	total number of QC/C						
	15	11	7	6	5	4	3
n-alkanes	3	2	2	2	2	1	1
iso-alkanes	6	4	3	2	1	1	1
aromatics	3	2	2	2	2	2	1
indanes/naphthalenes	1	1	0	0	0	0	0
cycloalkanes	1	1	0	0	0	0	0
olefins	1	1	0	0	0	0	0

Table 4

component	<i>n</i>	<i>A</i>	<i>B</i>	<i>C</i>	<i>D</i>
n-butane	4	-4.6402	4.850E2	1.340E-2	-1.970E-5
n-pentane	5	-7.1711	7.470E2	2.170E-2	-2.720E-5
n-hexane	6	-5.0715	6.550E2	1.230E-2	-1.50E-5
n-decane	10	-6.0716	1.020E3	1.220E-2	-1.190E-5
n-dodecane	12	-7.0687	1.263E3	1.3735E-2	-1.2215E-5

Table 5

group	carbon number	relative density ( $\tilde{\rho}$ )
n-alkanes	4	0.592
	5	0.631
	6	0.662
	10	0.737
	12	0.753
iso-alkanes	4	0.566
	5	0.620
	6	0.661
	7	0.691
	8	0.713
	9	0.729
	10	0.739
aromatics	8	0.884
	9	0.875
	10	0.872
	11	0.862
indanes/naphthalenes	9	0.969
cycloalkanes	8	0.771
olefins	9	0.733

Table 6

group	$A^*$	$a$	$\beta$	$\gamma$
n-/iso- alkanes	0.0035	1.2	0.5	0.167
aromatics	0.0346	1.2	1	0.167
indanes/naphthalenes	0.035	1.2	0.5	0.167
cycloalkanes	0.031	1.2	1	0.167
olefins	0.0361	1.2	1	0.167

Table 7

component	$n$	$A$	$B$	$T$	$T_c$
n-butane	4	33.0198	0.377	272.65	425.13
n-pentane	5	39.8543	0.398	309.22	469.65
n-hexane	6	45.610	0.401	341.88	507.43
n-decane	10	71.4282	0.451	447.30	618.45
n-dodecane	12	77.1658	0.407	489.47	658.20

Table 8

component	$n$	$A$	$B$	$C$	$D$
i-butane	4	-1.80770	258.930	0.003021	-8.64410E-06
C <sub>5</sub> H <sub>12</sub>	5	-5.80889	706.6875	0.014813	-1.85303E-05
C <sub>6</sub> H <sub>14</sub>	6	-10.2364	1387.157	0.024213	-2.40762E-05
C <sub>7</sub> H <sub>16</sub>	7	-4.84309	641.4304	0.011545	-1.37435E-05
C <sub>8</sub> H <sub>18</sub>	8	-10.2217	1423.586	0.024242	-2.33636E-05
C <sub>9</sub> H <sub>20</sub>	9	-4.25773	652.8668	0.008355	-8.98181E-06
C <sub>10</sub> H <sub>22</sub>	10	-4.8378	782.6433	0.009299	-9.37893E-06
C <sub>11</sub> H <sub>24</sub>	11	-4.23052	709.6763	0.007402	-7.41622E-06

Table 9

component	$n$	$A$	$B$
i-butane	4	31.95380	0.392
C <sub>5</sub> H <sub>12</sub>	5	37.68615	0.394981
C <sub>6</sub> H <sub>14</sub>	6	42.32119	0.389105
C <sub>7</sub> H <sub>16</sub>	7	46.95571	0.388222
C <sub>8</sub> H <sub>18</sub>	8	49.32456	0.382229
C <sub>9</sub> H <sub>20</sub>	9	56.10624	0.38
C <sub>10</sub> H <sub>22</sub>	10	59.25229	0.38
C <sub>11</sub> H <sub>24</sub>	11	65.11180	0.38

Table 10

component	$n$	$A$	$B$	$C$
o-xylene	8	0.28760	0.265130	0.27410
C <sub>9</sub> H <sub>12</sub>	9	0.269256	0.249881	0.274542
C <sub>10</sub> H <sub>14</sub>	10	0.276930	0.258413	0.288381
C <sub>11</sub> H <sub>16</sub>	11	0.275810	0.262610	0.285710

Table 11

component	$n$	$A$	$B$	$C$	$D$
o-xylene	8	-7.8805	1250.0	0.016116	-1.39930E-05
C <sub>9</sub> H <sub>12</sub>	9	-5.30135209	897.6554	0.009761	-8.86622E-06
C <sub>10</sub> H <sub>14</sub>	10	-4.346850	781.4415	0.007281	-6.73705E-06
C <sub>11</sub> H <sub>16</sub>	11	-4.6410	853.230	0.007850	-7.10120E-06

Table 12

Component	$n$	$A$	$B$
o-xylene	8	55.6060	0.3750
C <sub>9</sub> H <sub>12</sub>	9	59.97485694	0.38526
C <sub>10</sub> H <sub>14</sub>	10	63.32651773	0.379614
C <sub>11</sub> H <sub>16</sub>	11	65.20160	0.380

Table 13

group	<i>A</i>	<i>B</i>	<i>C</i>
indanes/naphthalenes	310.20	0.26114	0.30223
cycloalkanes	264.97	0.27385	0.28571
olefins	239.10	0.25815	0.28571

Table 14

group	<i>A</i>	<i>B</i>	<i>C</i>	<i>D</i>
indanes/naphthalenes	-7.3304	1330.6	0.0126170	-8.6008E-6
cycloalkanes	-4.2467	654.41	0.0085394	-9.3374E-6
olefins	-6.5557	993.50	0.0142320	-1.4097E-5

Table 15

group	<i>A</i>	<i>B</i>
indanes/naphthalenes	62.1067	0.42
cycloalkanes	50.9505	0.38
olefins	61.7073	0.38